Relative humidity control in polymer electrolyte membrane fuel cells without extra humidification

Luis A.M. Riascos*

Federal University of ABC, r. Santa Adelia 166, CEP 09210-170, Santo Andre, SP, Brazil

ARTICLE INFO

ABSTRACT

The performance of polymer electrolyte membrane fuel cells is highly influenced by the water content in the membrane. To prevent the membrane from drying, several researchers have proposed extra humidification on the input reactants. But in some applications, the extra size and weight of the humidifier should be avoided. In this research a control technique, which maintains the relative humidity on saturated conditions, is implemented by adjusting the air stoichiometry; the effects of drying of membrane and flooding of electrodes are considered, as well. For initial analysis, a mathematical model reveals the relationship among variables that can be difficult to monitor in a real machine. Also prediction can be tested optimizing time and resources. For instance, the effects of temperature and humidity can be analyzed separately. For experimental validation, tests in a fault tolerant fuel cell are conducted.

1. Introduction

Major efforts to reduce greenhouse gas emission have increased the demand for pollution-free energy sources. Fuel cells have attracted great attention in the recent years as a promising replacement for traditional stationary and mobile power sources. They are characterized by high power density, high efficiency and low emissions.

Significant improvements in polymer electrolyte membrane fuel cell (PEMFC) technology have been achieved over the past decade. However, the advances in performance, stability, reliability, and cost for today's fuel cell technology are not enough to replace internal combustion engines. A number of fundamental problems must be overcome to improve their performance and reduce their cost.

The design, control, and optimum operation of fuel cells require an understanding of their dynamics when changes in current, voltage, or power are requested. Also a control system is needed to ensure that humidity and temperature are within prescribed limits during operation, including conditions of variable loads.

The performance of a PEMFC is highly influenced by the water content in the membrane, which can be controlled through the relative humidity. In general, PEMFC with extra humidification of the input reactants work more efficiently [1]; however, in some applications, the extra size and weight of the humidifier should be avoided.

In this research a relative humidity control technique without extra humidification and based on the adjustment of the stoichiometry is implemented. Initially, the control technique is applied on a PEMFC model to analyze and to verify predictions about the system evolution. After that, tests are conducted for experimental validation of the simulation results.

This paper is organized as follows. In Section 2, the basic concepts for the mathematical model of a PEMFC are introduced. Section 3 introduces the proposed control technique and presents simulation tests. Section 4 presents tests for experimental validation and description of the experimental equipment. In Section 5 conclusions are emphasized.

2. The fuel cell model

Several mathematical models of PEMFC can be found in literature [1–4]. Basically a PEMFC model consists of an electrochemical and a thermo-dynamical part. In Ref. [2], an electrochemical model was introduced; in this case the polarization curve obtained with this model is compared to the polarization curve of the manufacturing data sheet to validate the model. In Ref. [5], the thermo-dynamical part of the model is introduced and the electrochemical part is extended to consider the effects of different types of faults.

2.1. The electrochemical model

The electrochemical model permits to calculate the cell voltage. The output voltage V_{FC} of a single cell can be defined as the result

* Tel.: +55 11 49963166; fax: +55 11 30915471.
E-mail address: luis.riascos@ufabc.edu.br.

Nomenclature

A	area of membrane (cm^2)
E_{Nernst}	open circuit voltage
FTFC	fault tolerant fuel cell
I_{FC}	electrical current of the FC (A)
J_{max}	maximum density of current (A cm^2)
J_n	fuel crossover (A cm^2)
ℓ	thickness of membrane (cm)
nr	number of cells
PEMFC	polymer electrolyte membrane fuel cell
P_{H_2}	hydrogen pressures (atm.)
P_{O_2}	oxygen pressures (atm.)
P_{sat}	saturated vapor pressure
P_W	partial pressure of water (atm).
Q_{gen}	generated heat (W)
RH	relative humidity
R_C	electrode resistance (Ω)
R_M	membrane resistance (Ω)
T	temperature
V_{act}	activation voltage drop
V_{con}	concentration voltage drop
V_{FC}	voltage of a single fuel cell
V_{ohmic}	ohmic voltage drop
V_s	stack voltage

Greek letter

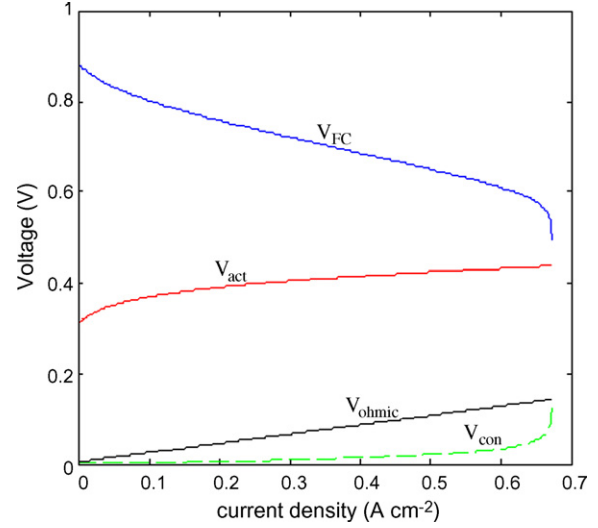|	
λ	air stoichiometric relationship

Fig. 1. Polarization curve.

V_{con} represents the voltage drop resulting from the mass transportation effects, which affects the concentration of the reacting gases:

$$V_{con} = -B \ln \left(1 - \frac{J}{J_{max}} \right) \qquad (6)$$

where B (V) is a constant depending on the type of cell, J_{max} is the maximum electric current density, and J is the electric current density produced by the cell. In general, $J = J_{out} + J_n$ where J_{out} is the real output electric current density, and J_n represents the fuel crossover and internal loss current.

Fig. 1 illustrates the polarization curve of a PEMFC applying the above electrochemical model.

Considering a stack composed by several cells, the output voltage can be assumed to be $V_S = nrV_{FC}$, where nr is the number of cells composing the stack. However, constructive characteristic of the stack such as flow distribution and heat transfer should be taken [6–10].

2.2. The thermo-dynamical model

The calculation of the relative humidity and the operating temperature essentially compose the thermo-dynamical model.

2.2.1. Temperature

The variation of temperature in the FC is obtained with the following differential equation [2]:

$$\frac{dT}{dt} = \frac{\Delta \dot{Q}}{MC_s} \qquad (7)$$

where M (kg) is the whole stack mass; C_s (J K^{-1} kg^{-1}) is the average specific heat coefficient of the stack; and $\Delta \dot{Q}$ is the rate of heat variation (i.e. the difference between heat generated and heat removed). Three types of heat removed are considered: heat by the reaction air flowing in the stack (Q_{rem1}), by the refrigeration system (Q_{rem2}), and heat exchanged with the surroundings (Q_{rem3}).

The rate of heat generated in the stack is calculated from the next equation [1]:

$$\dot{Q}_{gen} = Pow_s \left(\frac{1.48}{V_{FC}} - 1 \right) \qquad (8)$$

where Pow_s is the power produced by the stack.

of the following expression [1]:

$$V_{FC} = E_{Nernst} - V_{act} - V_{ohmic} - V_{con} \qquad (1)$$

E_{Nernst} represents the reversible open circuit voltage:

$$E_{Nernst} = 1.229 - 0.85 \times 10^{-3}(T - 298.15) + 4.31$$
$$\times 10^{-5}T \left[\ln(P_{H_2}) + \frac{1}{2} \ln(P_{O_2}) \right] \qquad (2)$$

where P_{H_2} and P_{O_2} (atm) are the hydrogen and oxygen pressures, respectively, and T (K) is the operating temperature.

V_{act} is the voltage drop due to the activation of the anode and the cathode:

$$V_{act} = -[\xi_1 + \xi_2 T + \xi_3 T \ln(c_{O_2}) + \xi_4 T \ln(I_{FC})] \qquad (3)$$

where ξ_i ($i = 1, \ldots, 4$) are specific coefficients for each type of cell, I_{FC} (A) is the electric current, and c_{O_2} (atm) is the oxygen concentration.

V_{ohmic} is the ohmic voltage drop associated with the conduction of protons through the solid electrolyte and electrons through the internal electronic resistance:

$$V_{ohmic} = I_{FC}(R_M + R_C) \qquad (4)$$

where R_C (Ω) is the resistance to electron flow, and R_M (Ω) is the resistance to proton transfer through the membrane:

$$R_M = \frac{\rho_M \ell}{A},$$
$$\rho_M = \frac{181.6 \cdot \left[1 + 0.03(I_{FC}/A) + 0.062(T/303)^2 (I_{FC}/A)^{2.5} \right]}{\left[\psi - 0.634 - 3(I_{FC}/A) \right] \exp[4.18(T - 303/T)]} \qquad (5)$$

where ρ_M (Ω cm) is the specific resistivity of membrane, ℓ (cm) is the membrane thickness, A (cm^2) is the active area of the membrane, and ψ is a specific coefficient for each type of membrane.

2.2.2. Relative humidity

The proton conductivity is directly proportional to the water content. Thus, there must be sufficient water content in the polymer electrolyte membrane.

In this research extra humidification of the input reactants is avoided. Then, dry hydrogen comes to the anode and air at environmental conditions comes to the cathode.

The chemical reactions forms water at the cathode, and because the membrane electrolyte is very thin, water would diffuse from the cathode side to the anode by back-diffusion during the operation of the cell. On the other hand, the hydrogen protons moving from the anode to the cathode pull water molecules with them by electro-osmotic drag. Fortunately, the more drag the more water production [11]. These combined effects are considered as the net water flux. In Refs. [12–14], the net water flux and other parameters are considered under several operational conditions.

The water production would keep the electrolyte hydrated. This level of hydration can be measured through the relative humidity of the output air. In practical applications, monitoring the relative humidity of the output air is a very simple and non-intrusive method to measure the relative humidity within the cell. In Ref. [15] several methods for monitoring the water content are discussed, but most can be applied only in laboratory conditions.

If the relative humidity is too low, then the membrane dries out and the conductivity decreases. In contrast, a relative humidity too high produces accumulation of liquid water on the electrodes, which can become flooded and block the pores; this makes gas diffusion difficult [14,16–19]. The result of these two constraints is a fairly narrow range of operating conditions.

To calculate the relative humidity of the output air, the balance of water is establishes:

output = input + internal generation

or in terms of the water partial pressure: $P_{W_{out}} = P_{W_{in}} + P_{W_{gen}}$.

And, also $RH_{out} \times P_{sat\_out} = P_{W_{out}}$.

then, the RH_{out} is

$$RH_{out} = \frac{P_{W_{in}} + P_{W_{gen}}}{P_{sat\_out}} \qquad (9)$$

where $P_{W_{in}}$ is the water partial pressure in the input air; $P_{W_{gen}}$ is the water partial pressure generated by the chemical reaction; P_{sat_out} is the saturated vapor pressure in the output air.

$$P_{W_{in}} = P_{sat\_in} RH_{in}$$

where RH_{in} is the relative humidity of the input air.

$P_{W_{gen}}$ is calculated from the next equation [2]:

$$P_{W_{gen}} = \frac{42.1 P_{air}}{\lambda - 0.188} \qquad (10)$$

where P_{air} is the air pressure (atm) and λ is the air stoichiometric relationship. The saturated vapor pressure (kPa) is calculated from the following equation:

$$P_{sat} = T^a \exp \frac{((b/T) + c)}{10} \qquad (11)$$

If $T > 273.15$ (K), then $a = -4.9283$; $b = -6763.28$; $c = 54.22$.

Fig. 2 illustrates the variation of temperature and relative humidity for constant air stoichiometry relationships, $\lambda = 2$, $\lambda = 4$, and $\lambda = 8$.

The air stoichiometry (λ) is calculated according to the following equation:

$$\lambda = \frac{42.1 P_{air}}{RH_{des} P_{sat\_out} - P_{W_{in}}} - 0.188 \qquad (12)$$
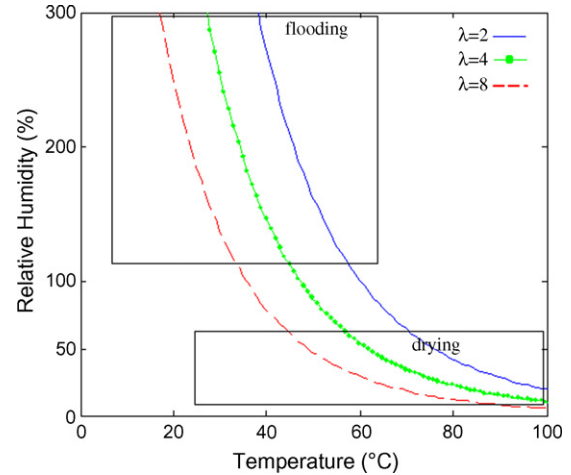

Fig. 2. Temperature and relative humidity for constant stoichiometries ($\lambda = 2$, 4, and 8).

where RH_{des} is the desired relative humidity to maintain saturated condition, normally between 80 and 100% [13].

To prevent the membrane from drying, several researchers have proposed extra humidification on the input reactants. In Ref. [1], several methods of extra humidification are described. In general, PEMFC with extra humidification works more efficiently, between 20 and 40% [12,20]. But in some applications (such as portable electronics), the extra size and weight of the humidifier should be avoided. In application of middle power PEMFC (about 5 kW) the humidification sections accounts for about 20% of the total volume and weight [12]. And most likely, the smaller plant the bigger humidifier. Also, some researches have reported other forms to avoid extra humidification [13,21,22].

Nevertheless, the operating conditions of the PEMFC are more sensitive to variation of the input air temperature than input relative humidity. The effects of temperature and relative humidity of the input air can be analyzed separately thanks to the PEMFC model. Fig. 3 illustrates the variation on the output RH produced by the adjustment on the input RH when input temperature is constant. In Ref. [13] a similar analysis is made considering RH_{in}, RH_{out}, and λ.

Another method to confirm the reduced effect of the input RH on the operating conditions of the PEMFC is to verify the limit operating temperature. The limit operating temperature is the temperature in which the PEMFC can operate preserving a
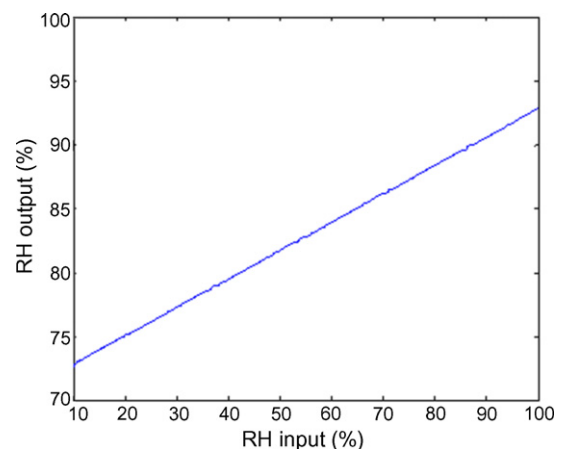

Fig. 3. Variation of RH_{output} vs. RH_{input}.
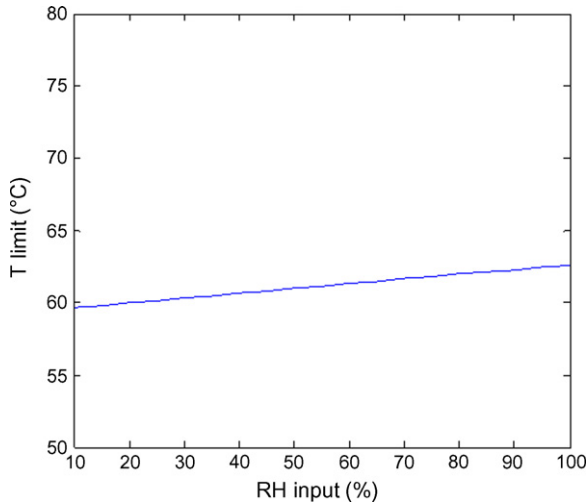
Fig. 4. Limit operating temperature vs. RH_{input}.

minimum recommended stoichiometry (in this case, $\lambda = 2$) and a recommended output RH (in this case, RH_{out} on saturated conditions). Fig. 4 illustrates the variation of the limit operating temperature obtained from combining Eqs. (11) and (12) when RH_{in} is modified and the temperature of the input air is constant ($T_{in} = 25\,°C$).

In contrast, Fig. 5 illustrates the variation of the limit operating temperature when T_{in} is modified and RH_{in} is constant ($RH_{in} = 50\%$). Actually, the water partial pressure of the air at $T = 60\,°C$ and $RH_{input} = 50\%$ is more than three times higher compared to this at $T = 25\,°C$ and $RH_{input} = 100\%$.

To prevent flooding problems, a common method for removing excess water inside the PEMFC is using the reaction air flowing through it. Air would be blown over the cathode, and apart from supplying the necessary oxygen it would dry out any excess water. The correct variation of the stoichiometry λ would maintain the RH proximal to saturated conditions.

The air stoichiometry influences both the availability of oxygen as well as the humidity of the membrane. A low stoichiometry limits the availability of oxygen because the air is depleted of oxygen when it reaches the end of the airflow channels. In Ref. [23], the effects on
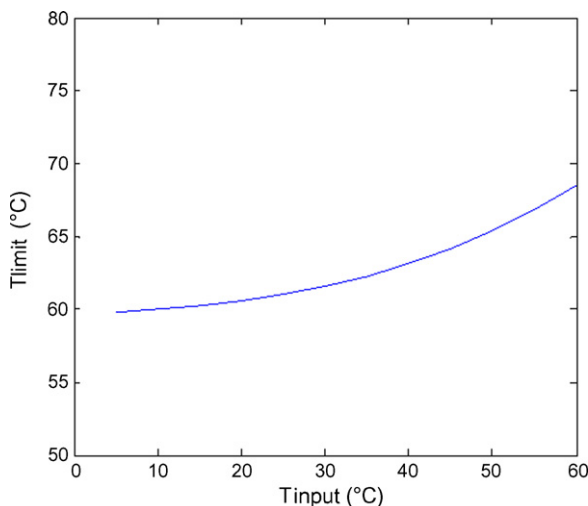
the PEMFC performance with different level of fuel utilization and air stoichometry utilization were tested. In general the maximum efficiency occurs at about 80% of fuel utilization (H_2) and 25% of air utilization.

The flooding of electrodes makes gas diffusion difficult and affects the performance of the PEMFC. This effect changes the resistance of electrodes (R_c), and is simulated applying the following equation [5]:

$$R_{c(k)} = R_{c(0)} \left(\frac{W_{acum(k)}}{const_1} \right)^{0.8} \tag{13}$$

where $R_{c(0)}$ is the electrode resistance at the initial state (normal condition), $const_1$ is a constant defining when the electrodes are led to flooding, and $W_{acum(k)}$ is the volume of water accumulated at instant k, $\dot{W}_{acum} = \dot{m}_{H_2O}(RH - 100\%)$. The rate of water production ($kg\,s^{-1}$) is calculated from the following equation [1]:

$$\dot{m}_{H_2O} = 9.34 \times 10^{-8} I_{FC} nr \tag{14}$$

This effect also can reduce the density of current; this reduction is simulated by the following equation [5]:

$$J_{max(k)} = \frac{J_{max(0)}}{(W_{acum(k)}/const_1)^{1.2}} \tag{15}$$

where $J_{max(0)}$ is the value of the maximum electric current density at the initial state (normal condition).

On the other hand, when temperature is higher than the limit operating temperature, the reacting air has a drying effect and reduces the RH. A low RH can produce a catastrophic effect on the polymer electrolyte membrane, which not only totally relies upon high water content, but also is very thin (and thus prone to rapid drying out). The drying of the membrane changes the resistance to proton flow (R_M). R_M is affected by the adjustment of ψ (see Eq. (5)); its variation is simulated according to the following equation [5]:

$$\psi_{(k)} = \frac{\psi_{(0)}}{(const_2/RH_{out(k)})^{1.12}} \tag{16}$$

where $\psi_{(0)}$ is the value at saturated condition, $RH_{out(k)}$ is the relative humidity of the output air at instant k, and $const_2$ is a constant defining when the membrane is led to drying.

Table 1 presents the parameters of the PEMFC in normal conditions.

In Ref. [24], a multi-parametric sensitivity analysis is performed to define the importance of the accuracy of each parameter. The accuracy was analyzed in normal conditions, considering variations around ±10% of their normal values.

Table 1
Parameters of the FC

Parameter	Value
nr	4
A	$62.5\,cm^2$
ℓ	$25\,\mu m$
P_{O_2}	$0.2095\,atm$
P_{H_2}	$1.47628\,atm$
$R_{C(0)}$	$0.003\,\Omega$
B	$0.015\,V$
ξ_1	-0.948
ξ_2	$0.00286 + 0.0002 \ln A + (4.3 \times 10^{-5}) \ln c_{H_2}$
ξ_3	7.22×10^{-5}
ξ_4	-1.06153×10^{-4}
$\psi_{(0)}$	23.0
J_n	$0.022\,A\,cm^2$
J_{max}	$0.672\,A\,cm^2$

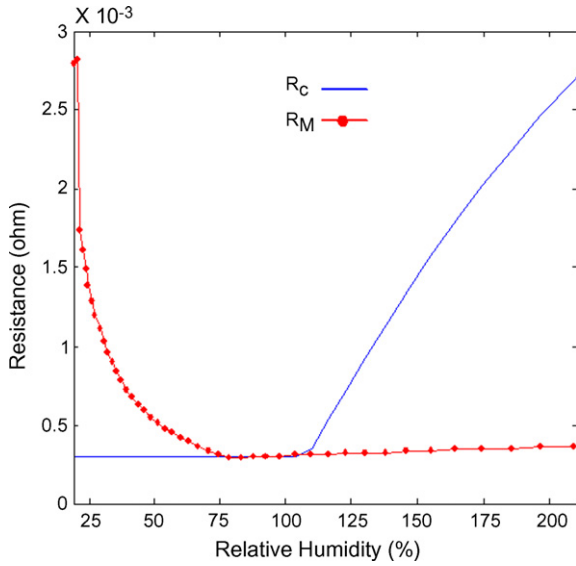**Fig. 5.** Limit operating temperature vs. T_{input}.

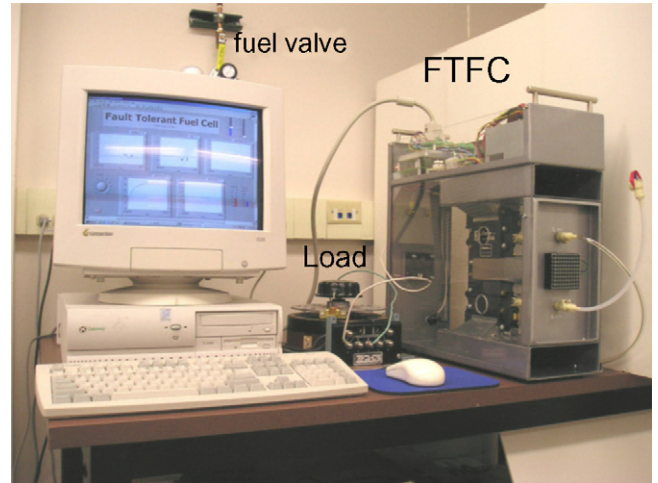Fig. 6. Effect of the relative humidity on the FC internal resistances.

Fig. 8. The FTFC.

Also, in Refs. [3,17] the variation of the resistances was associated with fault detection of flooding and drying.

Fig. 6 illustrates the influence of the relative humidity on the resistances according to Eqs. (15) and (16).

3. The fuel cell control technique

The proposed FC system adjusts the air stoichiometry to maintain humidity constantly on a saturated condition. However, in a real machine, there is not direct control on the stoichiometry, but there is direct control on the airflow.
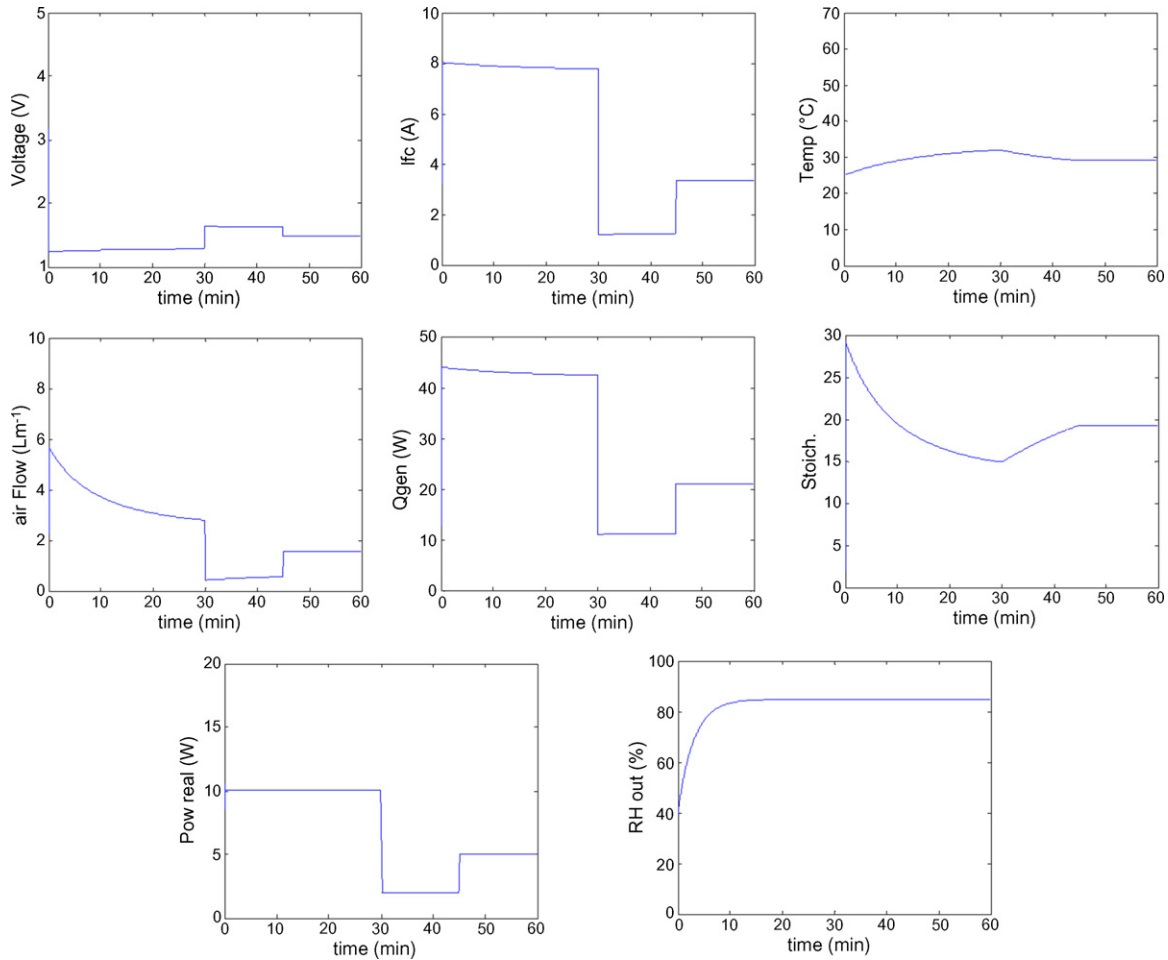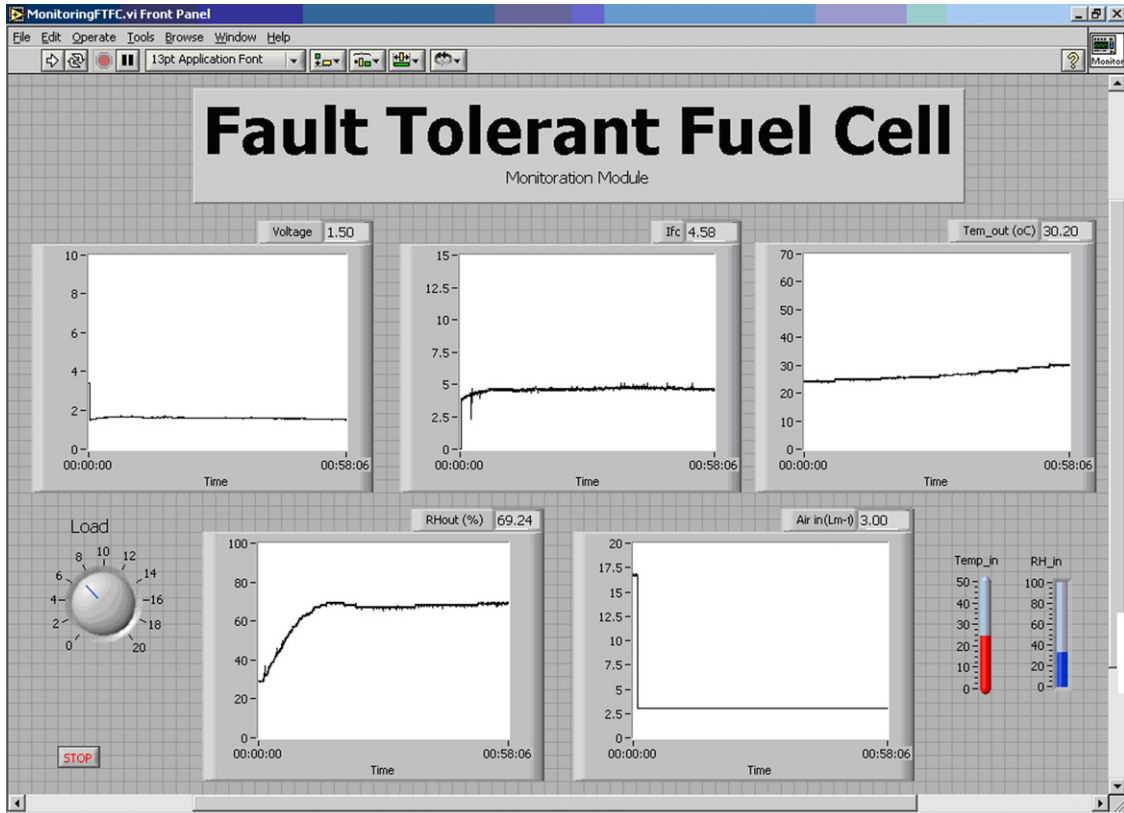

Fig. 7. Operation of the PEMFC.

Fig. 9. Monitoring of the FTFC applying LabView.

Applying Eq. (17) we calculate the reaction airflow ($L\,s^{-1}$) [1].

$$flow = 3.0238 \times 10^{-4} I_{FC\text{-}adj} nr \lambda \tag{17}$$

The electric current (I_{FC}) has been adjusted for considering internal loss current and fuel crossover (J_n).

In general, $I_{FC\text{-}adj} = I_{FC\text{-}real} + J_n A$.

$I_{FC\text{-}real}$ depends on the requested load, and nr is the number of cells (i.e. a constructive parameter). Therefore, the adjustment of the airflow is performed through the adjustment of λ according to Eq. (12).
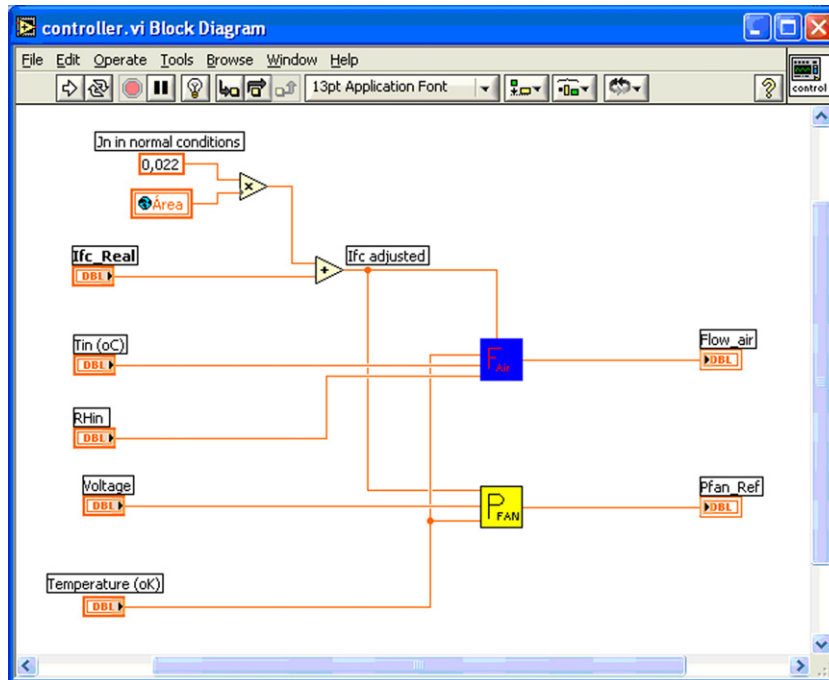

Fig. 10. Controller block diagram in LabView.

In the tests, air compressor and extra-humidification system are avoided. Then the air is considered with pressure of 1 atm and at environmental temperature (25 °C) and humidity (50%). Also the PEMFC system operates below the limit operating temperature. And the hydrogen supply is dead-end.

Before experimental validation, analysis on the PEMFC model was performed. The model is based on the equations of previous section and the parameters presented in Table 1. In Ref. [5] this model was applied to verify the effects of different types of faults, including drying and flooding.

Fig. 7 illustrates the evolution of the main PEMFC variables as a function of time. The variables are: voltage$_{stack}$ (V), electric current I_{FC} (A), temperature (°C), volume of airflow (L s^{-1}), generated heat (W), stoichiometry λ, power (W), and relative humidity. Initially in this simulation, the PEMFC supports a constant-load demand; thus, the voltage and current should adjust by themselves to supply this demand (i.e. the output power would be constant). And the control system adjusts the airflow to maintain the humidity on the desired value.

The simulation begins with the PEMFC system in stand-by (i.e. without load, and at environmental temperature, approximately 25 °C). After the load requirement is done, the electrical equilibrium is reached in less than 3 s (such as, the equilibrium of voltage and current). On the other hand, the temperature increases slowly as a consequence of a high inertia of the thermo-dynamical state. At $t = 30$ min, the thermo-dynamical state is almost stable, then step-variations of load are preformed at $t = 30$ and $t = 45$ min to analyze the transient response (variation of 20 and 50% of load, respectively); in these cases voltage and electric current are self-adjusted for the requested load, the airflow is adjusted by the control system, note that the RH$_{out}$ remains constant (85%).

4. Experimental validation

Key issues modeling PEM fuel cell systems are still developing, those include: lack of measurement techniques, especially real time (in situ) and non-intrusive techniques. More work is required in the areas of modeling, measurement methods and fuel cell design optimization [23].

A fault tolerant fuel cell (FTFC) was constructed at the PSERC laboratory [25,26]. The control system, the sensor system, and the power system compose the FTFC. The control system performs the adjustment of the airflow blower and the refrigeration blower. The sensor system implements the monitoring of voltage (V_S), electric current (I_{FC}), temperatures (T_{out} and T_{in}), and relative humidity (RH$_{out}$ and RH$_{in}$). The power system is composed by one AvistaLabs cartridge containing four polymer electrolyte membranes. The software LabView executes the control technique. The same LabView is applied for monitoring the variables and for controlling the speed of the blowers. The airflow is supplied by a brushless DC axial blower, nominal feed 12 VDC, maximum airflow 3 CFM (cubic feet per minute), operating voltage 5–13.8 VDC, maximum power 0.7 W, and maximum speed 4000 rpm. The hydrogen supply is dead-end with periodic manual purging to release impurities.

Fig. 8 illustrates the FTFC, the load, and a desktop computer with the software LabView executing the monitoring process. The constructive parameters of the FTFC are presented in Table 1.

Fig. 9 illustrates the graphic user interface of the panel control applying the LabView. This panel control presents several variables of the FTFC such as output voltage (V_S), electric current (I_{FC}), temperature, relative humidity (RH$_{out}$), and airflow volume. In Fig. 9 the FTFC begins to operate from stand-by and powering a constant load demand.

The control technique was implemented applying LabView; then the equations considered on previous sections should be translated to the LabView syntax. Fig. 10 illustrates the block diagram of the controller applying LabView. The inputs of the controller are: J_n, area, $I_{FC\text{-real}}$, T_{in}, RH$_{in}$, voltage, and T_{out}. Inside the F_{Air} block, Eqs. (12) and (17) are applied to calculate the air reaction flow. Inside the P_{FAN} block (power of the refrigeration fan) an empirical equation is applied to calculate the power of the refrigeration subsystem ($P_{fan\text{-Ref}}$). $P_{fan\text{-Ref}}$ depends on the voltage, $I_{FC\text{-adj}}$ and T_{out}.

Fig. 11 illustrates the inside of the F_{Air} block, basically in this block Eq. (17) is calculated and the power of the airflow blower is
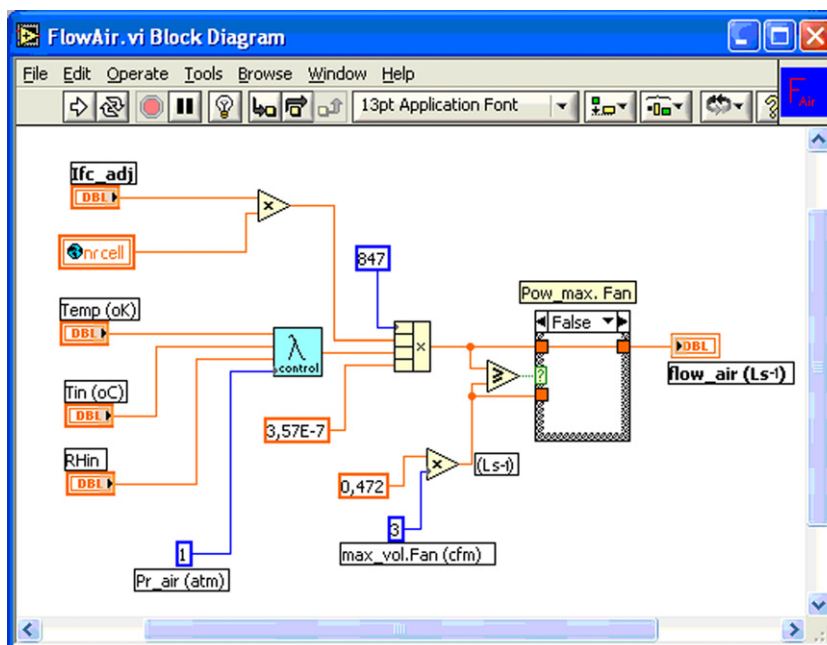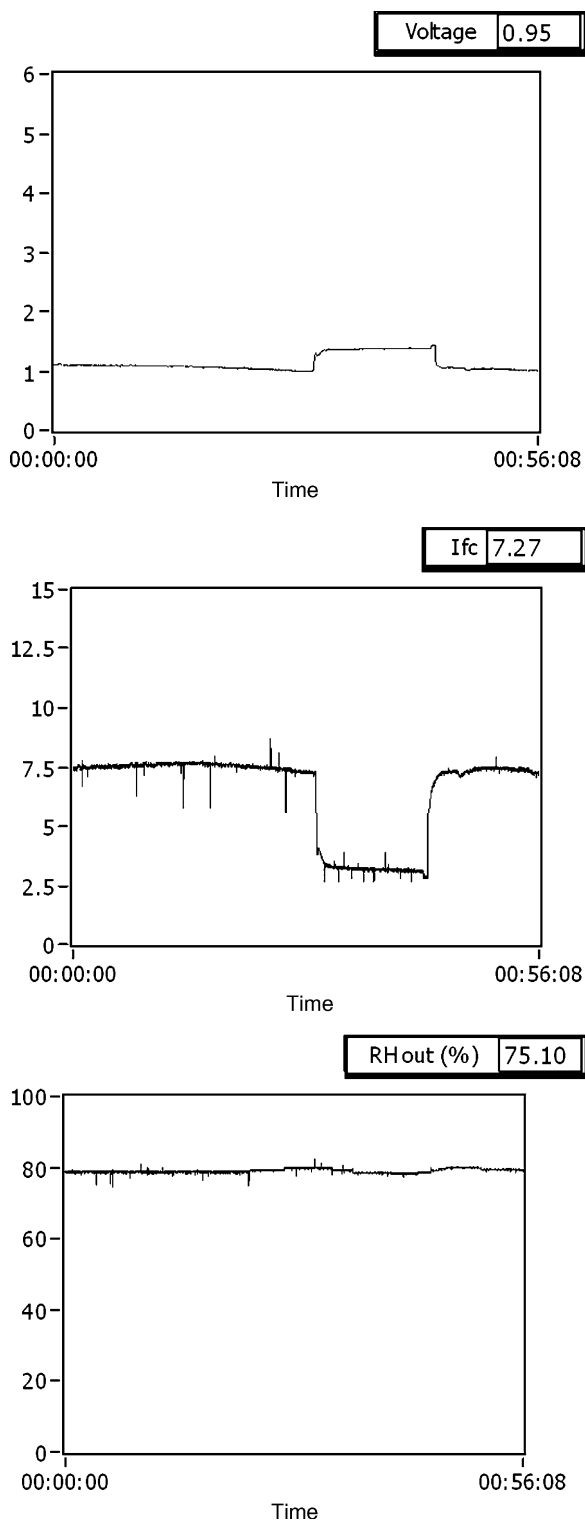

Fig. 11. F_{Air} block.

Fig. 12. Evolution of the FTFC variables under step load requirement.

lution of output voltage (V_S) and electric current (I_{FC}), and also how the controller maintains a constant relative humidity (RH_{out}).

5. Conclusions

The relative humidity is a crucial variable to improve the performance and to avoid damage to the membranes of PEMFC. A control technique, which maintains a satisfactory relative humidity, was implemented. This technique regulates the airflow adjusting the air stoichiometry and therefore maintains the relative humidity in a recommended value.

A PEMFC model was applied to analyze the evolution and to verify the dependence among the variables. From the mathematical model, the evolution of some variables that can be difficult to monitor in a real machine are observed (such as, generated heat, stoichiometry, portion of non-evaporated water, humidity over 100%, etc.). Also tests that can imply in permanent damage to the equipment can be avoided (such as, tests in very dry conditions).

In addition, predictions about the evolution of those variables can be tested, optimizing time and resources. The analysis in the PEMFC model shows that the relative humidity control strategy is stable and consistent under different operational conditions.

Experimental tests were conducted to verify the reliability of the proposed technique. The technique proved to be easy for implementation in the FTFC equipment.

Acknowledgments

References

[1] J. Larminie, A. Dicks, Fuel Cell Systems Explained, John Wiley & Sons Ltd., 2003.
[2] J.M. Correa, F.A. Farret, L.N. Canha, M.G. Simoes, IEEE Trans. Ind. Electron. 51 (5) (2004) 1103–1112.
[3] N. Fouquet, C. Doulet, C. Nouillant, G. Dauphin-Tanguy, B. Ould Bouamama, J. Power Sources 159 (2) (2006) 905–913.
[4] K. Promislow, B. Wetton, J. Power Sources 150 (4) (2005) 129–135.
[5] L.A.M. Riascos, M.G. Simoes, P.E. Miyagi, J. Power Sources 165 (1) (2007) 267–278.
[6] P.A.C. Chang, J. St-Pierre, J. Stumper, B. Wetton, J. Power Sources 162 (1) (2006) 340–355.
[7] S.A. Freunberger, M. Santis, I.A. Schneider, A. Wokaun, F.N. Büchi, J. Electrochem. Soc. 153 (2) (2006) A396–A405.
[8] S.A. Freunberger, M. Santis, I.A. Schneider, A. Wokaun, F.N. Büchi, J. Electrochem. Soc. 153 (5) (2006) A909–A913.
[9] M. Santis, S.A. Freunberger, M. Papra, A. Wokaun, F.N. Büchi, J. Power Sources 161 (2) (2006) 1076–1083.
[10] G.S. Kim, J. St-Pierre, K. Promislow, B. Wetton, J. Power Sources 152 (1) (2005) 210–217.
[11] X. Ren, S. Gottesfeld, J. Electrochem. Soc. 148 (1) (2001) A87–A93.
[12] F.N. Büchi, S. Srinivasan, J. Electrochem. Soc. 144 (8) (1997) 2767–2772.
[13] S.H. Chan, M. Han, S.P. Jiang, J. Electrochem. Soc. 154 (5) (2007) B486–B493.
[14] S.H. Ge, C.Y. Wang, J. Electrochem. Soc. 154 (10) (2007) B998–B1005.
[15] J. St-Pierre, J. Electrochem. Soc. 154 (7) (2007) B724–B731.
[16] C. Bao, M. Ouyanga, B. Yib, Int. J. Hydrogen Energy 31 (8) (2006) 1040–1057.
[17] J.M.L. Canut, R.M. Abouatallah, D.A. Harrington, J. Electrochem. Soc. 153 (5) (2006) A857–A864.
[18] H. Yamada, T. Hatanaka, H. Murata, Y. Morimoto, J. Electrochem. Soc. 153 (9) (2006) A1748–A1754.
[19] Z. Zhan, J. Xiao, D. Li, M. Pan, R. Yuan, J Power Sources 160 (2) (2006) 1041–1048.
[20] H. Yu, C. Ziegler, J. Electrochem. Soc. 153 (3) (2006) A570–A575.
[21] S.U. Jeong, A.E. Chob, H.J. Kimb, T.H. Limb, I.H. Ohb, S.H. Kima, J. Power Sources 159 (2006) 1089–1092.
[22] J. Tian, G. Sun, M. Cai, Q. Mao, Q. Xin, J. Electrochem. Soc. 155 (2) (2008) B187–B193.
[23] Q. Yan, H. Toghianib, H. Causeya, J. Power Sources 161 (1) (2006) 492–502.
[24] J.M. Correa, F.A. Farret, L.N. Canha, M.G. Simoes, V.A. Popov, IEEE Trans. Energy Convers. 20 (1) (2005) 211–218.
[25] L.A.M. Riascos, M.G. Simoes, F.G. Cozman, P.E. Miyagi, Bayesian network supervision on faults tolerant fuel cells, in: Proceedings of the 41st IEEE-IAS (Industry Application Society), Tampa, FL, USA, 2006.
[26] L.A.M. Riascos, M.G. Simoes, P.E. Miyagi, J. Power Sources 175 (1) (2007) 419–429.

limited by the maximum air volume, 3 CFM (cubic feet per minute). Eq. (12) is calculated inside the $\lambda_{control}$ block, in a similar method.

Before recording experimental test, the thermodynamic steady state was established. In Fig. 9 the evolution of the FTFC variables to reach the thermodynamic equilibrium was illustrated. After the equilibrium, the experimental test considering a step variation of load was conducted. In this test the load was reduced by 50% at $t = 30$ min, and reestablished at $t = 45$ min. Fig. 12 illustrates the evo-